
GRIP: ALGORITHM-AGNOSTIC MACHINE UNLEARNING FOR MIXTURE-OF-EXPERTS VIA GEOMETRIC ROUTER CONSTRAINTS

Andy Zhu
School of Computer Science
Georgia Institute of Technology*

Rongzhe Wei
School of Computer Science
Georgia Institute of Technology

Yupu Gu
Department of Electrical Engineering
Tsinghua University

Pan Li
School of Electrical and Computer Engineering
Georgia Institute of Technology *

ABSTRACT

Machine unlearning (MU) for large language models has become critical for AI safety, yet existing methods fail to generalize to Mixture-of-Experts (MoE) architectures. We identify that traditional unlearning methods exploit MoE’s architectural vulnerability: they manipulate routers to redirect queries away from knowledgeable experts rather than erasing knowledge, causing a loss of model utility and superficial forgetting. We propose Geometric Routing Invariance Preservation (GRIP), an algorithm-agnostic framework for unlearning for MoE. Our core contribution is a geometric constraint, implemented by projecting router gradient updates into an expert-specific null-space. Crucially, this decouples routing stability from parameter rigidity: while discrete expert selections remain stable for retained knowledge, the continuous router parameters remain plastic within the null space, allowing the model to undergo necessary internal reconfiguration to satisfy unlearning objectives. This forces the unlearning optimization to erase knowledge directly from expert parameters rather than exploiting the superficial router manipulation shortcut. GRIP functions as an adapter, constraining router parameter updates without modifying the underlying unlearning algorithm. Extensive experiments on large-scale MoE models demonstrate that our adapter eliminates expert selection shift (achieving over 95% routing stability) across all tested unlearning methods while preserving their utility. By preventing existing algorithms from exploiting MoE model’s router vulnerability, GRIP adapts existing unlearning research from dense architectures to MoEs.

1 Introduction

Large language models have achieved remarkable progress in the understanding and generation of natural language, transforming domains from scientific research to creative writing [1, 2, 3]. Despite their success, these models can often unintentionally memorize sensitive information from training data, including personal details, proprietary knowledge, and harmful content [4, 5, 6]. Machine unlearning (MU) has emerged as a potential solution to this vulnerability, providing mechanisms to selectively remove information from already trained models [7, 8, 9]. This capability is essential not only for regulatory compliance with privacy laws such as GDPR’s “right to be forgotten” [10, 11],

*azhu311@gatech.edu

but also for maintaining model safety by removing biased, outdated, or harmful knowledge post-deployment [12, 13].

While retraining from scratch provides the gold standard for machine unlearning, its computational cost has motivated the development of more efficient methods that manipulate model knowledge through targeted optimization [14, 15]. The majority of frontier approaches [16, 17, 18, 19, 20, 21, 22] share a core strategy of optimizing an unlearning objective (e.g., maximizing loss on forget data) to intentionally degrade performance on target data complemented with various methods to maintain general model capabilities. However, such methods targeting LLMs are primarily deployed and validated on dense architectures, assuming uniform parameter engagement for every input. This assumption is violated by the sparse models increasingly deployed at the frontier.

Recently, frontier LLMs have begun to primarily adopt sparse Mixture-of-Experts (MoE) architectures [23, 24, 25, 26]. In this architecture, each transformer layer contains multiple distinct feed-forward networks, or experts, and a router network that selects a small subset of these experts to process each input token, activating only a fraction of the model’s parameters per input. When applied to these models, existing unlearning methods fail catastrophically through expert selection shift [27]: rather than erasing knowledge from expert parameters, they manipulate routers to bypass knowledgeable experts. This routing disruption cascades through network depth as early-layer shifts alter representations flowing to later routers, causing severe utility degradation across all queries. Moreover, targeted information remains recoverable in bypassed experts, indicating superficial rather than genuine forgetting.

To this end, we propose *Geometric Routing Invariance Preservation (GRIP)*, an algorithm-agnostic framework that addresses this gap. GRIP introduces hard geometric constraints by projecting router gradient updates into subspaces that preserve routing decisions. Crucially, this formulation decouples routing stability from parameter rigidity; it forces the optimization to erase knowledge from expert parameters while allowing the router to dynamically adapt in directions orthogonal to the expert selecting vector of the retain set, preventing the model from becoming static.

To validate this framework, we conduct an extensive empirical evaluation on a 30 billion parameter MoE model, spanning hazardous knowledge removal (WMDP) and copyright protection (MUSE), ensuring broad applicability by testing GRIP across four distinct unlearning paradigms. We further rigorously probe the mechanism of unlearning through layer-wise routing analysis and adversarial expert forcing attacks, designed to determine whether knowledge is genuinely erased or merely hidden by router manipulation.

Our results demonstrate that GRIP eliminates the catastrophic trade-off observed in unconstrained baselines. We (i) restore routing stability from 0.21 to > 0.94 across all methods, (ii) improve retain accuracy by over 85% to match dense model baselines, and (iii) achieve genuine knowledge erasure where baselines fail by reducing adversarial knowledge recovery from 61% to just 3%. These gains are achieved with minimal computational overhead ($1.2\times$ training time) via our Post-Training Correction, establishing geometric constraints as a scalable, algorithm-agnostic solution for safe MoE deployment.

2 Related Work

Unlearning Methods for LLMs. Machine unlearning (MU) has recently gained significant attention for removing unwanted information from trained models without costly retraining [7, 9]. Existing methods approach this challenge through various optimization strategies. Many formulate unlearning as an objective, such as directly maximizing the loss on forget data via gradient ascent [14, 15], often regularized by a KL-divergence term against the original model to preserve retain set utility. Others leverage preference learning, such as Negative Preference Optimization (NPO), which trains the model to favor a generic, non-committal output over the specific information designated for removal [22, 21]. Alternatively, some methods intervene at the activation level; for instance, RMU (Representation Misdirection) identifies and nullifies internal representations that encode target knowledge [28, 29]. However, these methods are primarily designed with the assumption of a dense architecture. This assumption is violated by sparse MoEs, as their routers provide an optimization shortcut that these methods exploit. Consequently, the only prior work on MoE unlearning, SEUF [27], relies on soft regularization penalties and restricted expert updates, which risks incomplete

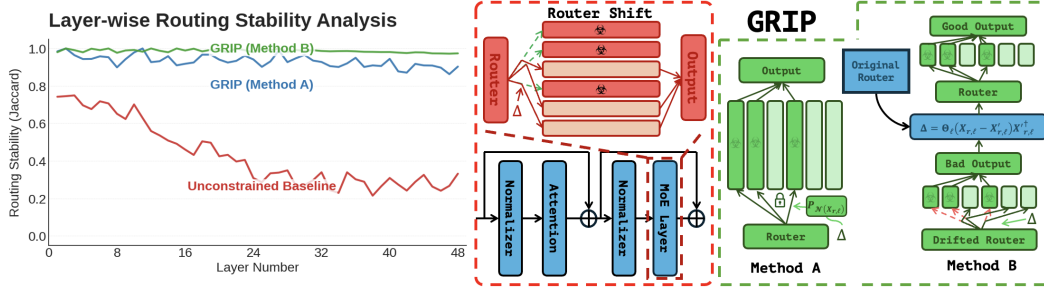


Figure 1: **Geometric Routing Invariance Preservation (GRIP) prevents expert selection collapse.** (a) The Problem: Standard unlearning methods suffer from Expert Selection Shift, where the router acts as an optimization shortcut, diverting queries away from knowledgeable experts rather than erasing information. This causes Routing Stability (RS), a measure of the consistency of expert selection we define formally in Eq (2), to collapse from 1.0 to ≈ 0.2 . (b) Our Solution: GRIP introduces two mechanisms to decouple routing stability from parameter plasticity: (a) Training-Time Enforcement, which projects gradients into a "safe" null-space orthogonal to the router’s decision boundaries; and (b) Post-Training Correction, which analytically realigns a drifted router after unlearning. Both methods restore stability to > 0.94 while preserving unlearning efficacy.

forgetting. Our framework, in contrast, addresses these limitations with hard geometric constraints that guarantee routing preservation while enabling comprehensive parameter updates.

The Rise of Mixture-of-Experts Architectures. Sparse MoE architectures have become ubiquitous in frontier LLMs, powering production systems such as Mixtral [25], DeepSeek-MoE [30], and GPT-4 [31]. This paradigm shift introduces the router network, a critical component governing expert selection that poses fundamental stability challenges for post-training modifications that do not exist in dense architectures.

MoE Routing Dynamics and Stability. The difficulty in modifying these routers stems from their operational significance. Recent research suggests that routing patterns encode semantic structure, with each expert specializing in specific syntactic roles, domains, or reasoning patterns [32, 33]. This makes routing preservation essential for maintaining model capabilities. While training-time stabilization is well-established [34, 23], our work is the first to formalize routing stability as a hard constraint for machine unlearning.

3 Preliminaries

Machine Unlearning. Given a model trained on an original dataset D_{train} , machine unlearning partitions this data into a forget set $D_f \subset D_{train}$ and a retain set $D_r = D_{train} \setminus D_f$. The objective is to produce updated model parameters that behave as if the model were trained exclusively on D_r . Our method operates on an N_r data point internal representation of this retain set at layer l , which we denote as the matrix $X_{r,l} \in \mathbb{R}^{d \times N_r}$ where d is the hidden dimension size of the router.

Mixture-of-Experts Layers. A sparse MoE layer processes an input representation $x_l \in \mathbb{R}^d$ at layer l using conditional computation, whereby only a fraction of the layer’s parameters are activated per input. The layer contains E expert networks and a router parameterized by $\Theta_l \in \mathbb{R}^{E \times d}$. For an input x_l , the router computes scores $s_l = \Theta_l x_l \in \mathbb{R}^E$ via linear projection and selects a subset of top- k experts, $\mathcal{S}_l(x_l; \Theta_l) \subseteq \{1, \dots, E\}$. The layer’s output is thus:

$$\sum_{j \in \mathcal{S}_l(x_l)} \frac{\exp(s_{l,j})}{\sum_{j' \in \mathcal{S}_l(x_l)} \exp(s_{l,j'})} \cdot \text{expert}_j(x_l) \quad (1)$$

where $\text{expert}_j(x_l)$ denotes the output of the j -th selected expert.

Expert Selection Shift and Routing Stability. During unlearning, gradient-based methods update router parameters $\Theta_l \rightarrow \Theta_l + \Delta\Theta_l$. This can induce *expert selection shift*, where the set of selected

experts post-unlearning, $\mathcal{S}_i^{\text{post}}(x)$, differs from the pre-unlearning set, $\mathcal{S}_i^{\text{pre}}(x)$. As discussed in Section 1, unlearning objectives can exploit this by manipulating $\Delta\Theta_i$ to redirect queries away from knowledgeable experts rather than erasing knowledge. Thus we quantify this effect using routing stability (RS), the Jaccard similarity between pre- and post-unlearning expert selections:

$$\text{RS}_i = \frac{1}{|\mathcal{Q}|} \sum_{x \in \mathcal{Q}} \frac{|\mathcal{S}_i^{\text{pre}}(x) \cap \mathcal{S}_i^{\text{post}}(x)|}{|\mathcal{S}_i^{\text{pre}}(x) \cup \mathcal{S}_i^{\text{post}}(x)|} \quad (2)$$

where \mathcal{Q} is the set of evaluation queries. An RS of 1 indicates perfect preservation, while 0 indicates complete routing collapse.

4 Methodology

While standard unlearning succeeds on dense models by optimizing over a static computation graph, MoEs introduce a dynamic dependency: the computation path itself is a function of the model parameters. This creates a dual optimization landscape where the unlearning objective can be minimized either by (1) genuinely erasing knowledge from expert weights, or (2) trivially altering the router to bypass them.

Standard gradient descent preferentially converges to the latter, creating an **optimization shortcut**. The gradient with respect to the router weights $\nabla_{\Theta} \mathcal{L}$ typically exhibits a larger expected norm than gradients for deep expert weights $\nabla_E \mathcal{L}$ due to the vanishing gradient effect through the sparse conditional computation graph. Furthermore, the router’s decision boundary is locally linear with respect to Θ , whereas expert outputs are highly non-linear deep functions. Consequently, a small perturbation $\|\Delta\Theta\| \ll \|\Delta E\|$ is sufficient to flip the selection indicator $\mathbb{I}[j \in \mathcal{S}_i(x)]$, effectively ‘hiding’ the forget set with minimal energy, corresponding to a steep descent direction in the loss landscape.

Figure 1(a) confirms this theoretical intuition: unconstrained optimization converges to this routing shortcut as router drift accumulates across network depth. Crucially, this failure is structural; minor representation drift in shallow layers ($\ell = 1-10$) alters the input manifold for deeper routers, invalidating their learned decision boundaries and triggering a cascading collapse. This observation dictates our design philosophy: effective MoE unlearning requires *decoupling* routing stability from parameter plasticity. Existing attempts to mitigate this via soft regularization, such as SEUF (Zhuang et al., 2025), prove insufficient; the steep gradient descent direction of the routing shortcut easily overwhelms soft penalties. Furthermore, as Zhuang et al. also identify, the alternative of strict parameter rigidity (freezing the router) fails to accommodate the necessary internal reconfigurations of the experts, leading to suboptimal unlearning. Thus, we must enforce stability geometrically by restricting updates to the subspace where routing decisions remain invariant while leaving orthogonal directions free for optimization.

To operationalize this, we present the GRIP framework. We first formalize routing preservation using null-space constraints (Section 4.1). Building off this, we develop a more flexible, expert-specific constraint decomposition (Section 4.2) and introduce two distinct methods for enforcing these constraints: a training-time projected gradient descent (Section 4.3) and an efficient post-training analytical correction (Section 4.4).

4.1 Null Space Constraints for Routing Preservation

We first formalize routing preservation by analyzing the effect of gradient updates on router parameters during unlearning. These updates can be decomposed into components that affect top-k selection and those that do not. For instance, modifications to expert scores well below the k -th ranked expert cannot influence routing. This observation motivates our approach of constraining updates to a “safe” subspace that preserves selection behavior, a concept we formalize using null-space constraints.

For retain representations $X_{r,\ell} \in \mathbb{R}^{N_r \times d}$ at layer ℓ , routing preservation requires identical top-k selections or more specifically $\mathcal{S}_\ell(X_{r,\ell}; \Theta_\ell + \Delta\Theta_\ell)$ to produce identical selections to $\mathcal{S}_\ell(X_{r,\ell}; \Theta_\ell)$. The most direct solution to guarantee this is to enforce zero change in all scores: $(\Theta_\ell + \Delta\Theta_\ell)X_{r,\ell} = \Theta_\ell X_{r,\ell}$, simplifying to $\Delta\Theta_\ell X_{r,\ell} = 0$. This characterizes the left null space of the input representations:

$$\mathcal{N}(X_{r,\ell}) = \{\Delta\Theta_\ell \in \mathbb{R}^{E \times d} : \Delta\Theta_\ell X_{r,\ell} = 0\} \quad (3)$$

We can thus re-parameterize router updates via projection onto this null-space to enforce selection constraints by construction. To construct this projector onto $\mathcal{N}(X_{r,\ell})$, we compute the eigendecomposition of the $d \times d$ feature covariance matrix, $X_{r,\ell}^T X_{r,\ell} = U_\ell \Lambda_\ell U_\ell^T$. Here, $U_\ell = [u_1, \dots, u_d]$ is the matrix of orthonormal eigenvectors and $\Lambda_\ell = \text{diag}(\lambda_1, \dots, \lambda_d)$ contains the corresponding eigenvalues.

We construct the null-space basis \hat{U}_ℓ from the eigenvectors, u_i , of the covariance matrix corresponding to negligible eigenvalues ($\lambda_i < \epsilon$). This defines the projector $P_{\mathcal{N}} = \hat{U}_\ell \hat{U}_\ell^T$, enabling the reparameterization $\Delta\Theta_\ell = W_\ell P_{\mathcal{N}}$. Importantly, this formulation decouples routing invariance from parameter plasticity. Since the router’s hidden dimension d exceeds the effective rank of the retained representations, the null space $\mathcal{N}(X_{r,\ell})$ remains high-dimensional. Consequently, the free variable W_ℓ retains significant capacity to optimize unlearning objectives in directions orthogonal to the retained subspace. This ensures that gradients driven by forget-set representations can freely alter the router’s behavior in these orthogonal directions, allowing the optimization to dismantle the specific routing pathways responsible for the forget set while strictly preserving the discrete top- k selection boundaries of the retain set.

However, strictly enforcing zero change in routing dynamics ($\Delta\Theta_\ell X_{r,\ell} \approx 0$) proves overly restrictive. Routing stability depends solely on relative score ordering, more specifically the integrity of the top- k selection, not absolute values. For instance, decreasing the score of a rank-50 expert does not alter the top- k selection, yet the global equality constraint prohibits this benign modification. This limitation necessitates a more granular, asymmetric formulation that enforces constraints only when parameter updates threaten to violate the specific inequality margins of the retained data.

4.2 Expert-Specific Constraint Decomposition

This observation motivates decomposing the global constraint into expert-specific formulations that respect each expert’s activation for each query. For expert j at layer l , we partition retain inputs by selection status, defining $\mathcal{I}_{j,l} = \{i : j \in \mathcal{S}_l(x_{r,l}^{(i)}; \Theta_l)\}$ as indices where expert j is selected. The asymmetric treatment yields the relaxed constraints:

$$(\Delta\Theta_l)_{j,:} x_{r,l}^{(i)} = 0 \quad \forall i \in \mathcal{I}_{j,l} \quad (4)$$

$$(\Delta\Theta_l)_{j,:} x_{r,l}^{(i)} \leq \tau_{i,j} \quad \forall i \notin \mathcal{I}_{j,l} \quad (5)$$

where $\tau_{i,j} = \min_{k \in \text{TopK}(x_{r,l}^{(i)})} [s_k - s_j]$ represents the margin to selection for routing scores s_k, s_j . These constraints operationalize the asymmetric treatment: constraint (4) is a hard equality constraint mandating zero score change for inputs $i \in \mathcal{I}_{j,l}$ that **selected** expert j , thus preserving critical model functionality. Conversely, constraint (5) is a relaxed inequality constraint for inputs $i \notin \mathcal{I}_{j,l}$ that did **not select** expert j . This formulation permits score modifications, provided the update $(\Delta\Theta_l)_{j,:} x_{r,l}^{(i)}$ remains below the selection margin $\tau_{i,j}$. It thus grants the optimization flexibility to modify non-selected expert parameters while strictly guaranteeing that the update does not inadvertently alter the original routing decision.

This expert-specific decomposition significantly expands the feasible optimization landscape compared to global constraints. By treating non-selected experts as inequality constraints rather than hard equalities (enforced via the projection algorithm in Section 4.3), we recover nearly the full gradient space, allowing for robust parameter updates while maintaining strict routing guarantees.

4.3 Training-Time Enforcement via Stochastic Projection

Unlike the global equality constraint, which admits a static closed-form solution, our expert-specific formulation introduces dynamic, input-dependent bounds that preclude enforcement via static reparameterization. Consequently, we employ a Projected Gradient Descent (PGD) framework that addresses the two distinct regimes of our constraints separately.

First, for the subset of inputs that *selected* expert j ($\mathcal{I}_{j,\ell}$), we require strict score preservation. We enforce this by defining a local, expert-specific null-space $\mathcal{N}(X_{\text{eq}}^{(j)})$, derived from the activating representations $X_{\text{eq}}^{(j)} = [x_{r,\ell}^{(i)}]_{i \in \mathcal{I}_{j,\ell}}$. By constructing the projector $P_{j,\ell}$ via the eigenvectors of $X_{\text{eq}}^{(j)}$

(analogous to Section 4.1), we ensure the gradient update remains strictly orthogonal to the subspace governing the existing routing scores.

However, for the non-selected inputs $x_{r,\ell}^{(i)}$, the router parameters Θ are constrained only to lie within dynamic half-spaces $\mathcal{H}_{i,j} = \{\Theta : \Theta x_{r,\ell}^{(i)} \leq \tau_{i,j} - \varepsilon\}$. This defines the full feasible region \mathcal{K} as the intersection of the equality subspace and these dynamic inequalities:

$$\mathcal{K} = \mathcal{N}(X_{\text{eq}}^{(j)}) \cap \bigcap_{i \notin \mathcal{I}_{j,\ell}} \mathcal{H}_{i,j} \quad (6)$$

Because the defining hyperplanes of $\mathcal{H}_{i,j}$ are functions of the input batch itself, \mathcal{K} varies with the data distribution, precluding the construction of a single, static projection operator. Furthermore, computing the exact Euclidean projection onto this polytope at each step requires solving a quadratic program with thousands of constraints (N_{ineq}), creating a prohibitive computational bottleneck. However, the projection onto any *single* constituent half-space $\mathcal{H}_{i,j}$ admits a closed-form solution. For a violated constraint, we seek the modified gradient $\tilde{\nabla}'$ that satisfies the constraint while minimizing deviation from the original optimization direction:

$$\tilde{\nabla}' = \underset{G}{\operatorname{argmin}} \|G - \tilde{\nabla}\|_F^2 \quad \text{s.t.} \quad \langle G, x_{r,\ell}^{(i)} \rangle = \tau_{i,j} - \varepsilon \quad (7)$$

To render enforcement tractable, we approximate the global projection onto \mathcal{K} via a stochastic process using Randomized Kaczmarz (RK). Rather than solving for the global intersection directly, we sample a single active constraint i at each iteration t with probability proportional to its geometric weight. The gradient is then updated using the closed-form solution to Equation (7):

$$\tilde{\nabla}^{(t+1)} = \tilde{\nabla}^{(t)} - \frac{\max(0, \langle \tilde{\nabla}^{(t)}, x_{r,\ell}^{(i)} \rangle - \tau_{i,j} + \varepsilon)}{\|x_{r,\ell}^{(i)}\|_2^2} x_{r,\ell}^{(i)} \quad (8)$$

This stochastic formulation functions as an unbiased estimator of the true projection while avoiding the cost of full polyhedral enforcement. We rely on the linear convergence guarantee established by [35], which bounds the expected error for consistent linear systems:

$$\mathbb{E}[\|\tilde{\nabla}^{(t)} - \tilde{\nabla}^*\|_2^2] \leq (1 - \kappa^{-2})^t \|\tilde{\nabla}^{(0)} - \tilde{\nabla}^*\|_2^2 \quad (9)$$

where $\kappa = \|X\|_F \|X^\dagger\|_2$ is the scaled condition number of the constraint matrix. In the context of MoE unlearning, the high-dimensionality of router inputs ($d \approx 4096$) yields a favorable condition number, ensuring that the error term decays exponentially. This allows us to enforce thousands of expert-specific constraints with high precision using only a small, fixed budget of iterations (k_{max}), avoiding the prohibitive computational cost of full second-order optimization.

4.4 Post-Training Analytical Correction

Training-time enforcement, while highly effective at preventing active router manipulation, faces a fundamental limitation in deep multi-layer models that undergo substantial parameter updates during unlearning: representation drift. As unlearning updates parameters in layers $1, \dots, \ell - 1$, the input representations $X_{r,\ell}$ shift to $X'_{r,\ell}$, rendering precomputed null-space projectors obsolete. However, rectifying this by continuously recomputing projectors necessitates $O(d^3)$ operations per update step, making exact constraint enforcement computationally prohibitive.

To address this, we introduce **Post-Training Correction (PTC)**, a deferred optimization strategy that explicitly decouples the unlearning objective from routing preservation. Instead of enforcing constraints online, we permit unconstrained optimization of the model parameters, followed by a single analytical projection that realigns the router weights to the shifted representations. Formally, given the post-unlearning shift $X_{r,\ell} \rightarrow X'_{r,\ell}$, we seek a correction $\Delta\Theta_\ell$ such that the original routing scores are restored: $(\Theta_\ell + \Delta\Theta_\ell)X'_{r,\ell} = \Theta_\ell X_{r,\ell}$. This yields the closed-form least-squares solution:

$$\Delta\Theta_\ell = \Theta_\ell (X_{r,\ell} - X'_{r,\ell}) X'_{r,\ell}{}^\dagger \quad (10)$$

where $X'_{r,\ell}{}^\dagger = X'_{r,\ell}{}^T (X'_{r,\ell} X'_{r,\ell}{}^T + \lambda I)^{-1}$ is the regularized pseudo-inverse with $\lambda = 10^{-6}$ (numerical stability details in Appendix D.5).

Table 1: Comprehensive evaluation across WMDP and MUSE benchmarks. \downarrow/\uparrow indicates lower/higher is better. Our methods are **bolded**. Router stability values calculate Jaccard similarity in expert selections using Equation (2)

Method	WMDP-Cyber			MUSE				
	FA \downarrow	RA \uparrow	RS \uparrow	C1 \downarrow	C2 \downarrow	C3 \downarrow	C4 \uparrow	RS \uparrow
Dense Baseline	0.28	0.70	N/A	17.0	25.0	43.5	44.6	N/A
GD	0.26	0.32	0.21	0.05	0.03	-25.6	4.31	0.26
Constrained + GD	0.24	0.51	0.94	0.04	0.02	-26.8	11.4	0.96
PTC + GD	0.26	0.55	0.99	0.01	0.00	-30.4	9.42	1.00
KL	0.28	0.35	0.42	15.3	22.9	-33.5	21.3	0.32
Constrained + KL	0.27	0.58	0.94	17.2	24.6	-30.1	42.7	0.96
PTC + KL	0.26	0.59	1.00	16.6	22.4	-32.9	41.8	1.00
NPO	0.33	0.48	0.45	16.3	22.1	-39.5	12.6	0.43
Constrained + NPO	0.29	0.62	0.97	15.3	23.8	-42.3	41.6	0.94
PTC + NPO	0.25	0.59	0.99	19.3	27.3	-46.1	41.2	1.00
RMU	0.26	0.35	0.43	0.00	0.01	-41.3	14.2	0.37
Constrained + RMU	0.24	0.65	0.96	0.02	0.00	-42.8	40.5	0.95
PTC + RMU	0.28	0.66	0.99	0.00	0.02	-41.9	39.2	1.00

The efficacy of this closed-form correction relies on the hypothesis that unlearning updates, while semantically significant, induce bounded perturbations in the representation space. Our empirical results (specifically the high recovery of Routing Stability in Table 1) validate this assumption, confirming that the representation drift $X_{r,\ell} \rightarrow X'_{r,\ell}$ sufficiently preserves the local topology to admit a linear realignment correction. While the global mapping of the model is highly non-linear, the representation drift $X_{r,\ell} \rightarrow X'_{r,\ell}$ preserves the local topology of the data manifold. Consequently, the router’s decision boundaries, linear hyperplanes in \mathbb{R}^d , do not need to be re-learned from scratch. Instead, they simply require **geometric realignment** to match the shifted input distribution.

This formulation fundamentally alters the efficiency profile by decoupling unlearning iterations (K) from projection operations. While training-time enforcement necessitates projections at every step, scaling as $\mathcal{O}(KLd^3)$, PTC requires only a single analytical correction per layer, reducing complexity to $\mathcal{O}(Ld^3)$. Since unlearning typically requires $K \geq 2000$ steps, this reduces the dominant overhead by three orders of magnitude, lowering the training penalty from $1.67\times$ to a negligible $1.21\times$. The associated storage cost $\mathcal{O}(LdN_r)$ is minor (≈ 0.5 GB for a 30B model). Furthermore, because the representations are static, we eliminate VRAM contention via an asynchronous pre-fetching strategy that streams $X_{r,\ell}$ from host memory only during the correction step.

We now proceed to an empirical validation of this post-training correction alongside the training-time enforcement (Section 4.3) to assess their efficacy in mitigating expert selection shift and preserving model utility.

5 Experimental Results

Datasets and Metrics. This method was applied to the Qwen3-30B-A3B model [36] and evaluate on the WMDP and MUSE benchmarks using standard protocols as detailed by their original papers (see Appendix A.1 for training details). We report Forget Accuracy (FA) and Retain Accuracy (RA) for the WMDP dataset and metrics C1 through C5 for the MUSE dataset as well as Routing Stability (RS) as defined in Eq. (2). A detailed breakdown of these metrics is located in Appendix (A.1).

5.1 Main Results

Our framework demonstrates substantial improvements across all metrics, particularly in routing stability and model utility preservation. Table 1 presents a comprehensive evaluation across multiple unlearning algorithms and benchmarks, revealing four key patterns that distinguish our approach from existing methods.

Significant Routing Stability Improvements. The primary result is the consistent achievement of near-perfect routing stability ($RS \geq 0.94$) across all base unlearning methods. Baseline approaches suffer severe routing disruption, with stability dropping as low as 0.21. Our post-training correction (PTC) consistently achieves **perfect or near-perfect stability (0.99-1.00)**, while online constraints maintain high stability (0.94-0.97). This represents a 350-400% relative improvement in routing preservation.

Superior Knowledge Retention. Our framework demonstrates substantial improvements in retain accuracy, with gains of 59%-94% relative to baseline methods. For instance, on WMDP-Cyber with RMU, retain accuracy improves from 0.35 to 0.65-0.66 (+85-88%). This improvement stems from our expert-specific constraint formulation that protects routing patterns for knowledge that should be preserved.

Maintained Unlearning Effectiveness. Critically, routing preservation does not compromise unlearning quality. Our methods achieve competitive or superior forget accuracy, with PTC+NPO reaching 0.25 on WMDP-Cyber (a 24% improvement over baseline NPO). This combination of high routing stability and effective forgetting indicates genuine knowledge erasure.

Dense-Level Utility Recovery. The bottom row of the table shows a baseline provided from the original paper of each metric performed on dense models (the exact models are detailed in Appendix A.1), demonstrating that our framework restores MoE models to dense-level performance. Our constrained MoE methods achieve utility preservation scores (40.5-44.6) that match or exceed MUSE’s best dense results. For instance, GA and NPO on dense models achieved 44.8-45.4 utility preservation on NEWS, while our Constrained+NPO reaches 44.6. This demonstrates complete recovery from unconstrained MoE performance degradation.

Table 2: Zero-Shot Utility Loss on General Benchmarks

Method	MMLU	TruthfulQA
Original Model	–	–
Baseline	-31%	-34%
Constrained	-10%	-11%
PTC	-14%	-12%

Performance on General Utility Benchmarks To verify general capability preservation beyond the retain set, we evaluated GRIP on MMLU and TruthfulQA in Table 2. GRIP recovers 86-90% of the original model’s zero-shot performance on the MMLU dataset and 88-89% on the TruthfulQA dataset, significantly outperforming unconstrained baselines which suffer catastrophic utility collapse.

5.2 Direct Comparison with SEUF

To provide a fair comparison with the state-of-the-art MoE unlearning framework SEUF [27], we evaluate on the same model architecture (Qwen1.5-MoE-A2.7B-Chat) using WMDP-Cyber (MUSE and WMDP-Bio evaluation is left out as SEUF was not originally evaluated on these datasets). As detailed in **Appendix F**, our framework substantially outperforms SEUF across all metrics. While achieving comparable forget accuracy (0.25–0.27 vs 0.25), we demonstrate superior retain accuracy (**0.61–0.63** vs 0.53, a 15–19% improvement) and routing stability (**0.94–0.99** vs 0.87, an 8–14% improvement).

Table 3: Expert forcing vulnerability on WMDP Dataset

Method	Normal FA↓	Forced FA↓	Vulnerability
Baseline	0.26	0.37	4.0×
SEUF	0.25	0.33	2.6×
GRIP	0.24	0.27	1.0×

5.3 Adversarial Evaluation via Expert Forcing

A critical distinction in machine unlearning is the difference between genuine information erasure and mere retrieval suppression. Recent work has demonstrated that standard unlearning often results

in "shallow alignment," where the model learns to suppress target knowledge via specific activation patterns rather than removing it from the weights [37]. Consequently, this "hidden" knowledge remains dormant and can be easily recovered via lightweight fine-tuning [38]. In MoE models, if the dangerous knowledge persists in the expert parameters, the safety mechanism is brittle: an adversary with white-box access can trivially bypass the router’s suppression logic [39] or manipulate internal activations to force the model into an unsafe state [40].

To quantify this vulnerability, we conduct expert forcing attacks that override the router’s post-unlearning decisions and forcefully access non-selected experts. For forget queries with routing shifts, we force generation through the top-5 non-selected experts. Table 3 shows baseline methods are **5.3×** more vulnerable than GRIP to knowledge extraction. This means one in six supposedly forgotten queries remains extractable in baseline approaches, while GRIP achieves near-zero recovery (3%), within noise margins. SEUF’s soft regularization only partially mitigates this vulnerability (4× higher than GRIP). These results validate that unconstrained methods exploit routing manipulation as an unintended shortcut, hiding knowledge rather than erasing it.

5.3.1 Implications for Security and Robustness

Vulnerability to Side-Channel Routing Inference. Our analysis suggests that routing patterns constitute a critical side-channel vulnerability for MoEs [41]. Even without parameter access, adversaries can infer expert selection through observable inference dynamics. In distributed MoE deployments, expert specialization often correlates with distinct latency profiles or memory access patterns [42]. An attacker can exploit this by monitoring API response times (Timing Attacks) to fingerprint which experts are active. If an unlearning method relies solely on redirecting queries to less knowledgeable experts an adversary can detect this redirection via latency shifts and craft perturbations to bypass the router’s fragile decision boundary. Unlike gradient-based extraction which requires white-box access, this routing inference operates under strictly weaker black-box assumptions [43], identifying a failure mode that is invisible to standard weight analysis.

Hardening Against Activation Steering. Beyond extraction, GRIP fundamentally hardens the model against activation steering attacks. Unconstrained unlearning degrades the router’s decision boundaries (Stability ≈ 0.21), creating a chaotic optimization landscape where small input perturbations can inadvertently flip expert selection back to unsafe regions. By enforcing geometric stability ($\Delta\Theta \approx 0$), GRIP locks the pre-trained decision boundaries, neutralizing steering attacks. Consequently, an adversary is forced to rely on *expert forcing* (manually activating erased experts) to recover knowledge. However, as demonstrated in our worst-case simulation (Section 5.3), GRIP effectively erases knowledge from the parameters themselves (3% recovery vs. 61% for baselines), rendering even this "nuclear option" ineffective.

Table 4: Ablation analysis of constraint methods

Constraint	FA↓	RA↑	RS↑	Rel. Time ↓
None (Baseline)	0.26	0.35	0.43	1.0×
Full Null Space	0.38	0.68	0.96	1.67×
Expert-Specific	0.24	0.65	0.96	1.71×
Post-Training	0.28	0.66	0.99	1.21×

5.4 Ablation Studies and Design Choices

To validate our design, we conducted an ablation study on different constraint formulations (Table 5) and a sensitivity analysis on the null-space threshold ϵ (Table 7).

Constraint Formulations. We evaluate our constraint designs in Table 4. The strict full null-space constraint ($\Delta\Theta X_r = 0$) successfully preserves routing (RS = 0.96) but overly restricts parameter plasticity, degrading unlearning effectiveness (FA = 0.45). Our Expert-Specific formulation resolves this trade-off, achieving superior erasure (FA = 0.24) while maintaining high stability (RS = 0.96).

While Post-Training Correction (PTC) yields the highest stability (RS = 0.99) and efficiency (1.21×), its unlearning performance lags slightly behind the Expert-Specific approach (FA = 0.28). This deficit highlights the critical role of Training-Time Enforcement: by permitting interim router drift,

PTC forces expert parameters to optimize against a non-stationary routing distribution, introducing gradient noise. Online enforcement eliminates this drift, providing a stable optimization landscape that allows experts to learn more precise unlearning representations. We therefore recommend the Expert-Specific formulation for maximum efficacy, reserving PTC for resource-constrained deployments.

Runtime Analysis Our Post-Training Correction (PTC) establishes a dominant operating point, achieving near-perfect routing stability (RS=0.99) with only a 1.21x training time overhead. In contrast, training time enforcement requires a 1.67x overhead to achieve comparable stability, highlighting PTC as the most efficient deployment strategy.

Table 5: Sensitivity Analysis of Null-Space Threshold ϵ

Threshold (ϵ)	RS (\uparrow)	FA (\downarrow)	RA (\uparrow)
10^{-4}	0.97	0.31	0.59
10^{-3}	0.96	0.28	0.62
10^{-2} (Default)	0.96	0.24	0.65
10^{-1}	0.89	0.25	0.59

Threshold Sensitivity Analysis. We further analyzed the sensitivity of the null-space threshold ϵ , testing values across four orders of magnitude ($\epsilon \in \{10^{-4}, 10^{-3}, 10^{-2}, 10^{-1}\}$). We utilize $\epsilon = 10^{-2}$ as the default for all experiments. As shown in Table 5, values orders of magnitude less than 10^{-2} proved overly restricted, resulting in empty null spaces in later layers and degraded unlearning performance (FA = 0.31). Conversely, overly loose thresholds (10^{-1}) lead to a drop in routing stability (0.89). The chosen value of 10^{-2} represents the optimal pareto frontier between stability and plasticity.

These comprehensive results establish our framework as a fundamental advancement for MoE model unlearning, providing consistent improvements across diverse benchmarks, unlearning algorithms, and evaluation metrics, demonstrating the broad applicability and robustness of our approach.

6 Future Work

Several promising directions emerge from this work. *Computational scalability* remains a key challenge: developing approximate projection techniques with sublinear complexity (e.g., randomized SVD, sketching methods) could enable better performance to models with thousands of experts and extremely high-dimensional routers. *Adaptive constraint mechanisms* that distinguish beneficial routing patterns from biased ones would allow selective modification of problematic routing behaviors while preserving legitimate specialization, which is critical for fairness-aware unlearning. *Fairness-Aware Routing* could explicitly address biased routing in retain-set data. GRIP can be extended to not only preserve all retain-set data by replacing the equality constraint with a 'fairness-aware' inequality constraint. For queries identified as triggering biased routing, the constraint would force the router to diverge from specific experts (e.g., $\Delta\Theta X > \epsilon$), effectively blending unlearning with alignment objectives

7 Conclusion

This work demonstrates that effective unlearning in Mixture-of-Experts models requires replacing soft regularization with hard geometric constraints. We find that standard gradient-based optimization on MoEs inevitably exploits the router as a shortcut, minimizing loss by shifting inputs rather than erasing knowledge from expert parameters. By projecting updates into the null space of the retain set's routing matrix, GRIP decouples routing stability from parameter plasticity, forcing the optimization to occur within the expert weights. Our analysis further identifies routing patterns as a distinct surface for adversarial manipulation. We show that even without parameter access, the specific routing shifts induced by unconstrained unlearning create observable side-channels that correlate with sensitive information. This implies that post-training modifications on sparse architectures must be explicitly "routing-aware" to prevent information leakage through inference dynamics.

Empirically, GRIP serves as an algorithm-agnostic framework compatible with existing unlearning methods. across a 30B-parameter model, it restores routing stability from 0.21 to >0.95 and reduces adversarial knowledge recovery from 61% to 3%, matching the efficacy of dense model baselines. These results establish that geometric constraints are a necessary and sufficient condition for preserving the structural integrity of MoEs during unlearning.

8 Limitations

Computational Requirements. Our approach requires storing retain-set representations $X_{r,\ell}$ across all layers, incurring $O(LdN_r)$ memory cost. For models with hundreds of layers or very large retain sets, this may become prohibitive. The post-training correction’s $O(d^3)$ complexity per layer, while more efficient than training-time enforcement, may also limit scalability to models with extremely high hidden dimensions.

Static Routing Assumption. While retain-set based routing restrictions exclusively constrains routers on beneficial behaviors, allowing for malicious router updates to be reverted, using purely Jaccard similarity as a metric does not account for the quality of routing decision, i.e. whether they are part of general model utility or born from malicious data.

Architectural Scope. Our method targets top- k token-choice MoE architectures. Alternative designs like expert-choice routing [34], soft MoE [44], or learned routing policies require adapted constraint formulations. While the geometric principles should generalize, specific implementations depend on the discrete top- k selection mechanism.

Verification Dilemma. By preserving routing patterns, GRIP makes unlearning operations undetectable through behavioral observation. Providers cannot easily audit unlearning success through routing analysis, necessitating alternative validation mechanisms like direct parameter inspection or membership inference attacks, which have their own limitations.

Acknowledgements

R. Wei and P. Li are partially supported by the NSF under awards PHY-2117997, IIS-2239565, IIS-2428777, and CCF-2402816; the JPMorgan Chase Faculty Award; and the OpenAI Researcher Access Program Credit, the Nvidia Academic Award, and the Google Academic Award.

References

- [1] Tom Brown, Benjamin Mann, Nick Ryder, Melanie Subbiah, Jared D Kaplan, Prafulla Dhariwal, Arvind Neelakantan, Pranav Shyam, Girish Sastry, Amanda Askell, Sandhini Agarwal, Ariel Herbert-Voss, Gretchen Krueger, Tom Henighan, Rewon Child, Aditya Ramesh, Daniel Ziegler, Jeffrey Wu, Clemens Winter, Chris Hesse, Mark Chen, Eric Sigler, Mateusz Litwin, Scott Gray, Benjamin Chess, Jack Clark, Christopher Berner, Sam McCandlish, Alec Radford, Ilya Sutskever, and Dario Amodei. Language models are few-shot learners. In H. Larochelle, M. Ranzato, R. Hadsell, M.F. Balcan, and H. Lin, editors, *Advances in Neural Information Processing Systems*, volume 33, pages 1877–1901. Curran Associates, Inc., 2020.
- [2] Hugo Touvron, Louis Martin, Kevin Stone, Peter Albert, Amjad Almahairi, Yasmine Babaei, Nikolay Bashlykov, Soumya Batra, Prajjwal Bhargava, Shruti Bhosale, Dan Bikel, Lukas Blecher, Cristian Canton Ferrer, Moya Chen, Guillem Cucurull, David Esiobu, Jude Fernandes, Jeremy Fu, Wenyin Fu, Brian Fuller, Cynthia Gao, Vedanuj Goswami, Naman Goyal, Anthony Hartshorn, Saghar Hosseini, Rui Hou, Hakan Inan, Marcin Kardas, Viktor Kerkez, Madian Khabsa, Isabel Kloumann, Artem Korenev, Punit Singh Koura, Marie-Anne Lachaux, Thibaut Lavril, Jenya Lee, Diana Liskovich, Yinghai Lu, Yuning Mao, Xavier Martinet, Todor Mihaylov, Pushkar Mishra, Igor Molybog, Yixin Nie, Andrew Poulton, Jeremy Reizenstein, Rashi Rungta, Kalyan Saladi, Alan Schelten, Ruan Silva, Eric Michael Smith, Ranjan Subramanian, Xiaoqing Ellen Tan, Binh Tang, Ross Taylor, Adina Williams, Jian Xiang Kuan, Puxin Xu, Zheng Yan, Iliyan Zarov, Yuchen Zhang, Angela Fan, Melanie Kambadur, Sharan Narang, Aurelien

- Rodriguez, Robert Stojnic, Sergey Edunov, and Thomas Scialom. Llama 2: Open foundation and fine-tuned chat models, 2023.
- [3] Gemini Team, Rohan Anil, Sebastian Borgeaud, Jean-Baptiste Alayrac, Jiahui Yu, Radu Soricut, Johan Schalkwyk, Andrew M. Dai, Anja Hauth, Katie Millican, David Silver, Melvin Johnson, Ioannis Antonoglou, Julian Schrittwieser, Amelia Glaese, Jilin Chen, Emily Pitler, Timothy Lillicrap, Angeliki Lazaridou, Orhan Firat, James Molloy, Michael Isard, Paul R. Barham, Tom Hennigan, Benjamin Lee, Fabio Viola, Malcolm Reynolds, Yuanzhong Xu, Ryan Doherty, Eli Collins, Clemens Meyer, Eliza Rutherford, Erica Moreira, Kareem Ayoub, Megha Goel, Jack Krawczyk, Cosmo Du, Ed Chi, Heng-Tze Cheng, Eric Ni, Purvi Shah, Patrick Kane, Betty Chan, Manaal Faruqui, Aliaksei Severyn, Hanzhao Lin, YaGuang Li, Yong Cheng, Abe Ittycheriah, Mahdis Mahdieh, Mia Chen, Pei Sun, Dustin Tran, Sumit Bagri, Balaji Lakshminarayanan, Jeremiah Liu, Andras Orban, Fabian Güra, Hao Zhou, Xinying Song, Aurelien Boffy, Harish Ganapathy, Steven Zheng, HyunJeong Choe, Ágoston Weisz, Tao Zhu, Yifeng Lu, Siddharth Gopal, Jarrod Kahn, Maciej Kula, Jeff Pitman, Rushin Shah, Emanuel Taropa, Majd Al Mery, Martin Bauml, Zhifeng Chen, Laurent El Shafey, Yujing Zhang, Olcan Sercinoglu, Becca Tucker, Enrique Piqueras, Maxim Krikun, Iain Barr, Nikolay Savinov, Ivo Danihelka, Becca Roelofs, Anaïs White, Anders Andreassen, Tamara von Glehn, Lakshman Yagati, Mehran Kazemi, Lucas Gonzalez, Misha Khalman, Jakub Sygnowski, Alexandre Frechette, Charlotte Smith, Laura Culp, Lev Proleev, Yi Luan, Xi Chen, James Lottes, Nathan Schucher, Federico Lebron, Alban Rustemi, Natalie Clay, Phil Crone, Tomas Kocisky, Jeffrey Zhao, Bartek Perz, Dian Yu, Heidi Howard, Adam Bloniarz, Jack W. Rae, Han Lu, Laurent Sifre, Marcello Maggioni, Fred Alcober, Dan Garrette, Megan Barnes, Shantanu Thakoor, Jacob Austin, Gabriel Barth-Maron, William Wong, Rishabh Joshi, Rahma Chaabouni, Deeni Fatiha, Arun Ahuja, Gaurav Singh Tomar, Evan Senter, Martin Chadwick, Ilya Kornakov, Nithya Attaluri, Iñaki Iturrate, Ruibo Liu, Yunxuan Li, Sarah Cogan, Jeremy Chen, Chao Jia, Chenjie Gu, Qiao Zhang, Jordan Grimstad, Ale Jakse Hartman, Xavier Garcia, Thanumalayan Sankaranarayanan Pillai, Jacob Devlin, Michael Laskin, Diego de Las Casas, Dasha Valter, Connie Tao, Lorenzo Blanco, Adrià Puigdomènech Badia, David Reitter, Mianna Chen, Jenny Brennan, Clara Rivera, Sergey Brin, Shariq Iqbal, Gabriela Surita, Jane Labanowski, Abhi Rao, Stephanie Winkler, Emilio Parisotto, Yiming Gu, Kate Olszewska, Ravi Addanki, Antoine Miech, Annie Louis, Denis Teplyashin, Geoff Brown, Elliot Catt, Jan Balaguer, Jackie Xiang, Pidong Wang, Zoe Ashwood, Anton Briukhov, Albert Webson, Sanjay Ganapathy, Smit Sanghavi, Ajay Kannan, Ming-Wei Chang, Axel Stjerngren, Josip Djolonga, Yuting Sun, Ankur Bapna, Matthew Aitchison, Pedram Pejman, Henryk Michalewski, Tianhe Yu, Cindy Wang, Juliette Love, Junwhan Ahn, Dawn Bloxwich, Kehang Han, Peter Humphreys, Thibault Sellam, James Bradbury, Varun Godbole, Sina Samangooei, Bogdan Damoc, and Alex Kaskasoli. Gemini: A Family of Highly Capable Multimodal Models. *arXiv e-prints*, page arXiv:2312.11805, December 2023.
- [4] Nicholas Carlini, Florian Tramèr, Eric Wallace, Matthew Jagielski, Ariel Herbert-Voss, Katherine Lee, Adam Roberts, Tom B. Brown, Dawn Xiaodong Song, Úlfar Erlingsson, Alina Oprea, and Colin Raffel. Extracting training data from large language models. In *USENIX Security Symposium*, 2020.
- [5] Chiyuan Zhang, Daphne Ippolito, Katherine Lee, Matthew Jagielski, Florian Tramèr, and Nicholas Carlini. Counterfactual memorization in neural language models. In *Thirty-seventh Conference on Neural Information Processing Systems*, 2023.
- [6] Milad Nasr, Javier Rando, Nicholas Carlini, Jonathan Hayase, Matthew Jagielski, A. Feder Cooper, Daphne Ippolito, Christopher A. Choquette-Choo, Florian Tramèr, and Katherine Lee. Scalable extraction of training data from aligned, production language models. In *The Thirteenth International Conference on Learning Representations*, 2025.
- [7] Lucas Bourtole, Varun Chandrasekaran, Christopher A. Choquette-Choo, Hengrui Jia, Adelin Travers, Baiwu Zhang, David Lie, and Nicolas Papernot. Machine unlearning. *2021 IEEE Symposium on Security and Privacy (SP)*, pages 141–159, 2019.
- [8] Yinzhi Cao and Junfeng Yang. Towards making systems forget with machine unlearning. In *2015 IEEE Symposium on Security and Privacy*, pages 463–480, 2015.
- [9] Thanh Tam Nguyen, Thanh Trung Huynh, Zhao Ren, Phi Le Nguyen, Alan Wee-Chung Liew, Hongzhi Yin, and Quoc Viet Hung Nguyen. A survey of machine unlearning. *ACM Trans. Intell. Syst. Technol.*, 16(5), September 2025.

- [10] European Parliament and Council of the European Union. Regulation (EU) 2016/679 of the European Parliament and of the Council of 27 April 2016 on the protection of natural persons with regard to the processing of personal data and on the free movement of such data, and repealing Directive 95/46/EC (General Data Protection Regulation), 2016.
- [11] Eduard Fosch Villaronga, Peter Kieseberg, and Tiffany Li. Humans forget, machines remember: Artificial intelligence and the right to be forgotten. *Computer Law Security Review*, 34(2):304–313, 2018.
- [12] Eric Mitchell, Charles Lin, Antoine Bosselut, Chelsea Finn, and Christopher D Manning. Fast model editing at scale. In *International Conference on Learning Representations*, 2022.
- [13] Laura Weidinger, John F. J. Mellor, Maribeth Rauh, Conor Griffin, Jonathan Uesato, Po-Sen Huang, Myra Cheng, Mia Glaese, Borja Balle, Atoosa Kasirzadeh, Zachary Kenton, Sande Minnich Brown, William T. Hawkins, Tom Stepleton, Courtney Biles, Abeba Birhane, Julia Haas, Laura Rimell, Lisa Anne Hendricks, William S. Isaac, Sean Legassick, Geoffrey Irving, and Iason Gabriel. Ethical and social risks of harm from language models. *ArXiv*, abs/2112.04359, 2021.
- [14] Joel Jang, Dongkeun Yoon, Sohee Yang, Sungmin Cha, Moontae Lee, Lajanugen Logeswaran, and Minjoon Seo. Knowledge unlearning for mitigating privacy risks in language models. In Anna Rogers, Jordan Boyd-Graber, and Naoaki Okazaki, editors, *Proceedings of the 61st Annual Meeting of the Association for Computational Linguistics (Volume 1: Long Papers)*, pages 14389–14408, Toronto, Canada, July 2023. Association for Computational Linguistics.
- [15] Jiaao Chen and Diyi Yang. Unlearn what you want to forget: Efficient unlearning for LLMs. In Houda Bouamor, Juan Pino, and Kalika Bali, editors, *Proceedings of the 2023 Conference on Empirical Methods in Natural Language Processing*, pages 12041–12052, Singapore, December 2023. Association for Computational Linguistics.
- [16] Yunzhi Yao, Peng Wang, Bozhong Tian, Siyuan Cheng, Zhoubo Li, Shumin Deng, Huajun Chen, and Ningyu Zhang. Editing large language models: Problems, methods, and opportunities. In Houda Bouamor, Juan Pino, and Kalika Bali, editors, *Proceedings of the 2023 Conference on Empirical Methods in Natural Language Processing*, pages 10222–10240, Singapore, December 2023. Association for Computational Linguistics.
- [17] Meghdad Kurmanji, Peter Triantafillou, Jamie Hayes, and Eleni Triantafillou. Towards unbounded machine unlearning. In *Proceedings of the 37th International Conference on Neural Information Processing Systems*, NIPS ’23, Red Hook, NY, USA, 2023. Curran Associates Inc.
- [18] Aditya Golatkar, Alessandro Achille, and Stefano Soatto. Eternal sunshine of the spotless net: Selective forgetting in deep networks. *2020 IEEE/CVF Conference on Computer Vision and Pattern Recognition (CVPR)*, pages 9301–9309, 2019.
- [19] Nathaniel Li, Alexander Pan, Anjali Gopal, Summer Yue, Daniel Berrios, Alice Gatti, Justin D. Li, Ann-Kathrin Dombrowski, Shashwat Goel, Long Phan, Gabriel Mukobi, Nathan Helm-Burger, Rassin Lababidi, Lennart Justen, Andrew B. Liu, Michael Chen, Isabelle Barrass, Oliver Zhang, Xiaoyuan Zhu, Rishub Tamirisa, Bhrrugu Bharathi, Adam Khoja, Zhenqi Zhao, Ariel Herbert-Voss, Cort B. Breuer, Samuel Marks, Oam Patel, Andy Zou, Mantas Mazeika, Zifan Wang, Palash Oswal, Weiran Lin, Adam A. Hunt, Justin Tienken-Harder, Kevin Y. Shih, Kemper Talley, John Guan, Russell Kaplan, Ian Steneker, David Campbell, Brad Jokubaitis, Alex Levinson, Jean Wang, William Qian, Kallol Krishna Karmakar, Steven Basart, Stephen Fitz, Mindy Levine, Ponnurangam Kumaraguru, Uday Tupakula, Vijay Varadharajan, Ruoyu Wang, Yan Shoshitaishvili, Jimmy Ba, Kevin M. Esvelt, Alexandr Wang, and Dan Hendrycks. The wmdp benchmark: Measuring and reducing malicious use with unlearning, 2024.
- [20] Jinghan Jia, Yihua Zhang, Yimeng Zhang, Jiancheng Liu, Bharat Runwal, James Diffenderfer, Bhavya Kailkhura, and Sijia Liu. SOUL: Unlocking the power of second-order optimization for LLM unlearning. In Yaser Al-Onaizan, Mohit Bansal, and Yun-Nung Chen, editors, *Proceedings of the 2024 Conference on Empirical Methods in Natural Language Processing*, pages 4276–4292, Miami, Florida, USA, November 2024. Association for Computational Linguistics.
- [21] Tomasz Korbak, Kejian Shi, Angelica Chen, Rasika Bhalerao, Christopher L. Buckley, Jason Phang, Samuel R. Bowman, and Ethan Perez. Pretraining language models with human preferences. In *Proceedings of the 40th International Conference on Machine Learning*, ICML’23. JMLR.org, 2023.

- [22] Ruiqi Zhang, Licong Lin, Yu Bai, and Song Mei. Negative preference optimization: From catastrophic collapse to effective unlearning. In *First Conference on Language Modeling*, 2024.
- [23] William Fedus, Barret Zoph, and Noam Shazeer. Switch transformers: scaling to trillion parameter models with simple and efficient sparsity. *J. Mach. Learn. Res.*, 23(1), January 2022.
- [24] Nan Du, Yanping Huang, Andrew M Dai, Simon Tong, Dmitry Lepikhin, Yuanzhong Xu, Maxim Krikun, Yanqi Zhou, Adams Wei Yu, Orhan Firat, Barret Zoph, Liam Fedus, Maarten P Bosma, Zongwei Zhou, Tao Wang, Emma Wang, Kellie Webster, Marie Pellat, Kevin Robinson, Kathleen Meier-Hellstern, Toju Duke, Lucas Dixon, Kun Zhang, Quoc Le, Yonghui Wu, Zhifeng Chen, and Claire Cui. GLaM: Efficient scaling of language models with mixture-of-experts. In Kamalika Chaudhuri, Stefanie Jegelka, Le Song, Csaba Szepesvari, Gang Niu, and Sivan Sabato, editors, *Proceedings of the 39th International Conference on Machine Learning*, volume 162 of *Proceedings of Machine Learning Research*, pages 5547–5569. PMLR, 17–23 Jul 2022.
- [25] Albert Q Jiang, Alexandre Sablayrolles, Arthur Mensch, Chris Bamford, Devendra S Chaplot, Diego de las Casas, Florian Bressand, Gianna Lengyel, Guillaume Lample, Lucile Saulnier, et al. Mixtral of experts. *arXiv preprint arXiv:2401.04088*, 2024.
- [26] Damai Dai, Chengqi Deng, Chenggang Zhao, R.x. Xu, Huazuo Gao, Deli Chen, Jiashi Li, Wangding Zeng, Xingkai Yu, Y. Wu, Zhenda Xie, Y.k. Li, Panpan Huang, Fuli Luo, Chong Ruan, Zhifang Sui, and Wenfeng Liang. DeepSeekMoE: Towards ultimate expert specialization in mixture-of-experts language models. In Lun-Wei Ku, Andre Martins, and Vivek Srikumar, editors, *Proceedings of the 62nd Annual Meeting of the Association for Computational Linguistics (Volume 1: Long Papers)*, pages 1280–1297, Bangkok, Thailand, August 2024. Association for Computational Linguistics.
- [27] Haomin Zhuang, Yihua Zhang, Kehan Guo, Jinghan Jia, Gaowen Liu, Sijia Liu, and Xiangliang Zhang. SEUF: Is unlearning one expert enough for mixture-of-experts LLMs? In Wanxiang Che, Joyce Nabende, Ekaterina Shutova, and Mohammad Taher Pilehvar, editors, *Proceedings of the 63rd Annual Meeting of the Association for Computational Linguistics (Volume 1: Long Papers)*, pages 8664–8678, Vienna, Austria, July 2025. Association for Computational Linguistics.
- [28] Nathaniel Li, Alexander Pan, Anjali Gopal, Summer Yue, Daniel Berrios, Alice Gatti, Justin D. Li, Ann-Kathrin Dombrowski, Shashwat Goel, Gabriel Mukobi, Nathan Helm-Burger, Rassin Lababidi, Lennart Justen, Andrew Bo Liu, Michael Chen, Isabelle Barrass, Oliver Zhang, Xiaoyuan Zhu, Rishub Tamirisa, Bhrugu Bharathi, Ariel Herbert-Voss, Cort B Breuer, Andy Zou, Mantas Mazeika, Zifan Wang, Palash Oswal, Weiran Lin, Adam Alfred Hunt, Justin Tienken-Harder, Kevin Y. Shih, Kemper Talley, John Guan, Ian Steneker, David Campbell, Brad Jokubaitis, Steven Basart, Stephen Fitz, Ponnurangam Kumaraguru, Kallol Krishna Karmakar, Uday Tupakula, Vijay Varadharajan, Yan Shoshitaishvili, Jimmy Ba, Kevin M. Esvelt, Alexandr Wang, and Dan Hendrycks. The WMDP benchmark: Measuring and reducing malicious use with unlearning. In *Forty-first International Conference on Machine Learning*, 2024.
- [29] Andy Zou, Long Phan, Sarah Chen, James Campbell, Phillip Guo, Richard Ren, Alexander Pan, Xuwang Yin, Mantas Mazeika, Ann-Kathrin Dombrowski, Shashwat Goel, Nathaniel Li, Michael J. Byun, Zifan Wang, Alex Mallen, Steven Basart, Sanmi Koyejo, Dawn Song, Matt Fredrikson, J. Zico Kolter, and Dan Hendrycks. Representation engineering: A top-down approach to ai transparency, 2025.
- [30] DeepSeek-AI, Aixin Liu, Bei Feng, Bing Xue, Bingxuan Wang, Bochao Wu, Chengda Lu, Chenggang Zhao, Chengqi Deng, Chenyu Zhang, Chong Ruan, Damai Dai, Daya Guo, Dejian Yang, Deli Chen, Dongjie Ji, Erhang Li, Fangyun Lin, Fucong Dai, Fuli Luo, Guangbo Hao, Guanting Chen, Guowei Li, H. Zhang, Han Bao, Hanwei Xu, Haocheng Wang, Haowei Zhang, Honghui Ding, Huajian Xin, Huazuo Gao, Hui Li, Hui Qu, J. L. Cai, Jian Liang, Jianzhong Guo, Jiaqi Ni, Jiashi Li, Jiawei Wang, Jin Chen, Jingchang Chen, Jingyang Yuan, Junjie Qiu, Junlong Li, Junxiao Song, Kai Dong, Kai Hu, Kaige Gao, Kang Guan, Kexin Huang, Kuai Yu, Lean Wang, Lecong Zhang, Lei Xu, Leyi Xia, Liang Zhao, Litong Wang, Liyue Zhang, Meng Li, Miaojun Wang, Mingchuan Zhang, Minghua Zhang, Minghui Tang, Mingming Li, Ning Tian, Panpan Huang, Peiyi Wang, Peng Zhang, Qiancheng Wang, Qihao Zhu, Qinyu Chen, Qiushi Du, R. J. Chen, R. L. Jin, Ruiqi Ge, Ruisong Zhang, Ruizhe Pan, Runji Wang, Runxin Xu, Ruoyu Zhang, Ruyi Chen, S. S. Li, Shanghao Lu, Shangyan Zhou, Shanhuang Chen, Shaoqing Wu, Shengfeng Ye, Shengfeng Ye, Shirong Ma, Shiyu Wang, Shuang Zhou, Shuiping Yu, Shunfeng Zhou, Shuting Pan, T. Wang, Tao Yun, Tian Pei, Tianyu Sun, W. L. Xiao, Wangding Zeng,

Wanjia Zhao, Wei An, Wen Liu, Wenfeng Liang, Wenjun Gao, Wenqin Yu, Wentao Zhang, X. Q. Li, Xiangyue Jin, Xianzu Wang, Xiao Bi, Xiaodong Liu, Xiaohan Wang, Xiaojin Shen, Xiaokang Chen, Xiaokang Zhang, Xiaosha Chen, Xiaotao Nie, Xiaowen Sun, Xiaoxiang Wang, Xin Cheng, Xin Liu, Xin Xie, Xingchao Liu, Xingkai Yu, Xinnan Song, Xinxia Shan, Xinyi Zhou, Xinyu Yang, Xinyuan Li, Xuecheng Su, Xuheng Lin, Y. K. Li, Y. Q. Wang, Y. X. Wei, Y. X. Zhu, Yang Zhang, Yanhong Xu, Yanhong Xu, Yanping Huang, Yao Li, Yao Zhao, Yaofeng Sun, Yaohui Li, Yaohui Wang, Yi Yu, Yi Zheng, Yichao Zhang, Yifan Shi, Yiliang Xiong, Ying He, Ying Tang, Yishi Piao, Yisong Wang, Yixuan Tan, Yiyang Ma, Yiyuan Liu, Yongqiang Guo, Yu Wu, Yuan Ou, Yuchen Zhu, Yudian Wang, Yue Gong, Yuheng Zou, Yujia He, Yukun Zha, Yunfan Xiong, Yunxian Ma, Yuting Yan, Yuxiang Luo, Yuxiang You, Yuxuan Liu, Yuyang Zhou, Z. F. Wu, Z. Z. Ren, Zehui Ren, Zhangli Sha, Zhe Fu, Zhean Xu, Zhen Huang, Zhen Zhang, Zhenda Xie, Zhengyan Zhang, Zhewen Hao, Zhibin Gou, Zhicheng Ma, Zhigang Yan, Zhihong Shao, Zhipeng Xu, Zhiyu Wu, Zhongyu Zhang, Zhuoshu Li, Zihui Gu, Zijia Zhu, Zijun Liu, Zilin Li, Ziwei Xie, Ziyang Song, Ziyi Gao, and Zizheng Pan. DeepSeek-V3 Technical Report. *arXiv e-prints*, page arXiv:2412.19437, December 2024.

- [31] OpenAI, Josh Achiam, Steven Adler, Sandhini Agarwal, Lama Ahmad, Ilge Akkaya, Florencia Leoni Aleman, Diogo Almeida, Janko Altschmidt, Sam Altman, Shyamal Anadkat, Red Avila, Igor Babuschkin, Suchir Balaji, Valerie Balcom, Paul Baltescu, Haiming Bao, Mohammad Bavarian, Jeff Belgum, Irwan Bello, Jake Berdine, Gabriel Bernadett-Shapiro, Christopher Berner, Lenny Bogdonoff, Oleg Boiko, Madelaine Boyd, Anna-Luisa Brakman, Greg Brockman, Tim Brooks, Miles Brundage, Kevin Button, Trevor Cai, Rosie Campbell, Andrew Cann, Brittany Carey, Chelsea Carlson, Rory Carmichael, Brooke Chan, Che Chang, Fotis Chantzis, Derek Chen, Sully Chen, Ruby Chen, Jason Chen, Mark Chen, Ben Chess, Chester Cho, Casey Chu, Hyung Won Chung, Dave Cummings, Jeremiah Currier, Yunxing Dai, Cory Decareaux, Thomas Degry, Noah Deutsch, Damien Deville, Arka Dhar, David Dohan, Steve Dowling, Sheila Dunning, Adrien Ecoffet, Atty Eleti, Tyna Eloundou, David Farhi, Liam Fedus, Niko Felix, Simón Posada Fishman, Juston Forte, Isabella Fulford, Leo Gao, Elie Georges, Christian Gibson, Vik Goel, Tarun Gogineni, Gabriel Goh, Rapha Gontijo-Lopes, Jonathan Gordon, Morgan Grafstein, Scott Gray, Ryan Greene, Joshua Gross, Shixiang Shane Gu, Yufei Guo, Chris Hallacy, Jesse Han, Jeff Harris, Yuchen He, Mike Heaton, Johannes Heidecke, Chris Hesse, Alan Hickey, Wade Hickey, Peter Hoeschele, Brandon Houghton, Kenny Hsu, Shengli Hu, Xin Hu, Joost Huizinga, Shantanu Jain, Shawn Jain, Joanne Jang, Angela Jiang, Roger Jiang, Haozhun Jin, Denny Jin, Shino Jomoto, Billie Jonn, Heewoo Jun, Tomer Kaftan, Łukasz Kaiser, Ali Kamali, Ingmar Kanitscheider, Nitish Shirish Keskar, Tabarak Khan, Logan Kilpatrick, Jong Wook Kim, Christina Kim, Yongjik Kim, Jan Hendrik Kirchner, Jamie Kiros, Matt Knight, Daniel Kokotajlo, Łukasz Kondraciuk, Andrew Kondrich, Aris Konstantinidis, Kyle Kosic, Gretchen Krueger, Vishal Kuo, Michael Lampe, Ikai Lan, Teddy Lee, Jan Leike, Jade Leung, Daniel Levy, Chak Ming Li, Rachel Lim, Molly Lin, Stephanie Lin, Mateusz Litwin, Theresa Lopez, Ryan Lowe, Patricia Lue, Anna Makanju, Kim Malfacini, Sam Manning, Todor Markov, Yaniv Markovski, Bianca Martin, Katie Mayer, Andrew Mayne, Bob McGrew, Scott Mayer McKinney, Christine McLeavey, Paul McMillan, Jake McNeil, David Medina, Aalok Mehta, Jacob Menick, Luke Metz, Andrey Mishchenko, Pamela Mishkin, Vinnie Monaco, Evan Morikawa, Daniel Mossing, Tong Mu, Mira Murati, Oleg Murk, David Mély, Ashvin Nair, Reiichiro Nakano, Rajeev Nayak, Arvind Neelakantan, Richard Ngo, Hyeonwoo Noh, Long Ouyang, Cullen O’Keefe, Jakub Pachocki, Alex Paino, Joe Palermo, Ashley Pantuliano, Giambattista Parascandolo, Joel Parish, Emy Parparita, Alex Passos, Mikhail Pavlov, Andrew Peng, Adam Perelman, Filipe de Avila Belbute Peres, Michael Petrov, Henrique Ponde de Oliveira Pinto, Michael, Pokorny, Michelle Pokrass, Vitchyr H. Pong, Tolly Powell, Alethea Power, Boris Power, Elizabeth Proehl, Raul Puri, and Alec Radford. GPT-4 Technical Report. *arXiv e-prints*, page arXiv:2303.08774, March 2023.
- [32] Suchin Gururangan, Margaret Li, Mike Lewis, Weijia Shi, Tim Althoff, Noah A. Smith, and Luke Zettlemoyer. Scaling expert language models with unsupervised domain discovery. *ArXiv*, abs/2303.14177, 2023.
- [33] Barret Zoph, Irwan Bello, Sameer Kumar, Nan Du, Yanping Huang, Jeff Dean, Noam Shazeer, and William Fedus. St-moe: Designing stable and transferable sparse expert models, 2022.
- [34] Yanqi Zhou, Tao Lei, Hanxiao Liu, Nan Du, Yanping Huang, Vincent Y. Zhao, Andrew Dai, Zhifeng Chen, Quoc Le, and James Laudon. Mixture-of-experts with expert choice routing. In

- Proceedings of the 36th International Conference on Neural Information Processing Systems, NIPS '22*, Red Hook, NY, USA, 2022. Curran Associates Inc.
- [35] Thomas Strohmer and Roman Vershynin. A randomized kaczmarz algorithm with exponential convergence, 2007.
 - [36] Jin Xu, Zhifang Guo, Hangrui Hu, Yunfei Chu, Xiong Wang, Jinzheng He, Yuxuan Wang, Xian Shi, Ting He, Xinfu Zhu, Yuanjun Lv, Yongqi Wang, Dake Guo, He Wang, Linhan Ma, Pei Zhang, Xinyu Zhang, Hongkun Hao, Zishan Guo, Baosong Yang, Bin Zhang, Ziyang Ma, Xipin Wei, Shuai Bai, Keqin Chen, Xuejing Liu, Peng Wang, Mingkun Yang, Dayiheng Liu, Xingzhang Ren, Bo Zheng, Rui Men, Fan Zhou, Bowen Yu, Jianxin Yang, Le Yu, Jingren Zhou, and Junyang Lin. Qwen3-omni technical report, 2025.
 - [37] Anonymous. Erase or hide? suppressing spurious unlearning neurons for robust unlearning. In *Submitted to The Fourteenth International Conference on Learning Representations*, 2025. under review.
 - [38] Anonymous. Unlearning isn't deletion: Investigating reversibility of machine unlearning in LLMs. In *Submitted to The Fourteenth International Conference on Learning Representations*, 2025. under review.
 - [39] Xiangyu Qi, Yi Zeng, Tinghao Xie, Pin-Yu Chen, Ruoxi Jia, Prateek Mittal, and Peter Henderson. Fine-tuning aligned language models compromises safety, even when users do not intend to! In *The Twelfth International Conference on Learning Representations*, 2024.
 - [40] Krishna Kanth Nakka, Xue Jiang, Dmitrii Usynin, and Xuebing Zhou. PII jailbreaking in LLMs via activation steering reveals personal information leakage. In *Mechanistic Interpretability Workshop at NeurIPS 2025*, 2025.
 - [41] Yifan Zhou, Tianshi Xu, Jue Hong, Ye Wu, and Meng Li. Cryptomoe: Privacy-preserving and scalable mixture of experts inference via balanced expert routing. In *The Thirty-ninth Annual Conference on Neural Information Processing Systems*, 2025.
 - [42] Zibo Gao, Junjie Hu, Feng Guo, Yixin Zhang, Yinglong Han, Siyuan Liu, Haiyang Li, and Zhiqiang Lv. I know what you said: unveiling hardware cache side-channels in local large language model inference. In *Proceedings of the 34th USENIX Conference on Security Symposium, SEC '25*, USA, 2025. USENIX Association.
 - [43] Itay Yona, Iliia Shumailov, Jamie Hayes, and Nicholas Carlini. Stealing user prompts from mixture of experts, 2024.
 - [44] Joan Puigcerver, Carlos Riquelme Ruiz, Basil Mustafa, and Neil Houlsby. From sparse to soft mixtures of experts. In *The Twelfth International Conference on Learning Representations*, 2024.
 - [45] Weijia Shi, Jaechan Lee, Yangsibo Huang, Sadhika Malladi, Jieyu Zhao, Ari Holtzman, Daogao Liu, Luke Zettlemoyer, Noah A. Smith, and Chiyuan Zhang. MUSE: Machine unlearning six-way evaluation for language models. In *The Thirteenth International Conference on Learning Representations*, 2025.

A Implementation Details

Our experiments were conducted using the PyTorch framework, leveraging Hugging Face's transformers and accelerate libraries for efficient model handling and distributed training.

Model Architecture We use **Qwen3-MoE-30B-A3B**, a custom variant of the Qwen model family with a Mixture-of-Experts architecture comprising 128 experts per MoE layer, with a top-8 routing strategy. The model has approximately 3 billion active parameters during inference.

Hardware and Quantization All unlearning procedures were executed on a single node equipped with **2 NVIDIA H200 80GB GPUs** and a single node equipped with **8 NVIDIA L40s 40GB GPUs**. To maximize throughput and reduce the memory footprint, we employed **FP8 precision** for both weights and activations during the unlearning steps. Specifically, we utilized the E4M3 floating-point format, which is well-suited for training stability, and integrated NVIDIA's TransformerEngine library to handle the FP8 mixed-precision logic seamlessly.

Hyperparameters The unlearning process for our proposed method and all baselines was configured with the hyperparameters listed in Table 6, chosen via a preliminary sweep on a held-out validation set.

Table 6: Hyperparameters for all unlearning experiments.

Hyperparameter	Value
Optimizer	AdamW
Learning Rate	3×10^{-5}
Batch Size (per GPU)	2
Adam β_1	0.9
Adam β_2	0.999
Adam ϵ	1×10^{-8}
Weight Decay	0.01
Maximum Unlearning Steps	10000

A.1 Evaluation Metric Details

WMDP Metrics.

- **Forget Accuracy (FA):** The accuracy of the model on multiple-choice questions (MCQA) derived from the hazardous corpora (Bio/Cyber). Lower is better (approaching random guess ≈ 0.25).
- **Retain Accuracy (RA):** The accuracy on MMLU and general knowledge MCQA tasks. Higher is better (approaching original model performance).

MUSE Metrics. We adhere to the four-way categorization defined by [45]:

- **C1 (Verbatim Memorization):** Measures the Rouge-L overlap of model completions given prefixes from the target book. Unlearning aims to minimize this (Lower is better).
- **C2 (Knowledge Probing):** Accuracy on MCQA probing specific facts about the book’s plot and characters (Lower is better).
- **C3 (Privacy Leakage):** Measures the model’s tendency to output specific proper nouns (entity extraction) associated with the copyrighted text (Lower is better).
- **C4 (Local Hallucination):** Measures the consistency of the model on unrelated texts. We report the preservation rate (Higher is better).

A.2 Unlearning Baseline Formulations

To ensure fair comparison, we standardized the loss functions for all baseline methods used in Section 5. Let $f_\theta(x)$ denote the model output and \mathcal{L}_{CE} denote the cross-entropy loss.

Gradient Ascent (GA). We maximize the loss on the forget set D_f while optionally minimizing loss on the retain set D_r (simulated via gradient accumulation or replay).

$$\mathcal{L}_{GA} = -\mathcal{L}_{CE}(f_\theta(x_f), y_f) + \alpha \mathcal{L}_{CE}(f_\theta(x_r), y_r) \quad (11)$$

KL Minimization (KL). We minimize the KL divergence between the unlearned model and a fixed reference model (the initial pre-trained model θ_{ref}) on the forget set, encouraging the model to output a uniform or "refusal" distribution.

$$\mathcal{L}_{KL} = \text{KL}(f_{\theta_{ref}}(x_f) || f_\theta(x_f)) + \mathcal{L}_{CE}(f_\theta(x_r), y_r) \quad (12)$$

Negative Preference Optimization (NPO). Following [22], we treat the forget data as a negative preference sample. The objective makes the forget likelihood worse than the reference model while remaining bounded:

$$\mathcal{L}_{NPO} = -\log \sigma \left(\beta \log \frac{\pi_\theta(y_f|x_f)}{\pi_{\theta_{ref}}(y_f|x_f)} - \beta \log \tau \right) \quad (13)$$

where β controls the strength of the penalty and τ is a margin hyperparameter.

Representation Misdirection (RMU). Following [19], we perturb the internal activations $h_l(x_f)$ of the model at layer l to match a random target vector v_{rand} , preventing the extraction of semantic knowledge:

$$\mathcal{L}_{RMU} = \|h_l(x_f) - v_{rand}\|_2^2 \quad (14)$$

B Null Space Projection Construction

We provide the detailed construction of the null space projector $P_{\mathcal{N}(X_{r,\ell})}$ used in Section 4.1.

B.1 Eigen-decomposition Method

Given retain-set representations $X_{r,\ell} \in \mathbb{R}^{d \times N_r}$ at layer ℓ , we compute the covariance matrix:

$$C_\ell = X_{r,\ell} X_{r,\ell}^T \in \mathbb{R}^{d \times d} \quad (15)$$

We perform eigendecomposition of C_ℓ :

$$C_\ell = U_\ell \Lambda_\ell U_\ell^T \quad (16)$$

where $U_\ell = [u_1, u_2, \dots, u_d] \in \mathbb{R}^{d \times d}$ contains orthonormal eigenvectors and $\Lambda_\ell = \text{diag}(\lambda_1, \lambda_2, \dots, \lambda_d)$ contains eigenvalues ordered as $\lambda_1 \geq \lambda_2 \geq \dots \geq \lambda_d \geq 0$.

The null space of $X_{r,\ell}$ corresponds to eigenvectors with zero (or near-zero) eigenvalues. In practice, we use a threshold $\epsilon = 10^{-2}$ to identify null space eigenvectors:

$$\hat{U}_\ell = [u_i : \lambda_i < \epsilon] \in \mathbb{R}^{d \times k} \quad (17)$$

where $k = |\{i : \lambda_i < \epsilon\}|$ is the dimension of the approximate null space.

The null space projector is then:

$$P_{\mathcal{N}(X_{r,\ell})} = \hat{U}_\ell \hat{U}_\ell^T \quad (18)$$

For any gradient $\nabla \in \mathbb{R}^{E \times d}$, the projected gradient $\tilde{\nabla} = P_{\mathcal{N}(X_{r,\ell})} \nabla$ satisfies $\tilde{\nabla} X_{r,\ell} \approx 0$ within numerical precision.

B.2 Parameterization for Unconstrained Optimization

The null space projector can be used to reparameterize router updates. Instead of optimizing $\Delta\Theta_\ell$ directly with constraints, we can optimize an unconstrained matrix $W_\ell \in \mathbb{R}^{E \times d}$ and set:

$$\Delta\Theta_\ell = P_{\mathcal{N}(X_{r,\ell})} W_\ell \quad (19)$$

This ensures $\Delta\Theta_\ell \in \mathcal{N}(X_{r,\ell})$ by construction, eliminating the need for explicit constraint enforcement. However, as discussed in Section 4.1, this approach is overly restrictive for MoE routing.

B.3 Computational Complexity

The eigendecomposition of $C_\ell \in \mathbb{R}^{d \times d}$ requires $O(d^3)$ operations. This is performed once per layer before unlearning begins. Storing $\hat{U}_\ell \in \mathbb{R}^{d \times k}$ requires $O(dk)$ memory, where typically $k \approx d - N_r$ for full-rank $X_{r,\ell}$.

Applying the projection to a gradient $\nabla \in \mathbb{R}^{E \times d}$ requires:

$$\tilde{\nabla} = \hat{U}_\ell (\hat{U}_\ell^T \nabla) \in O(Edk) \quad (20)$$

For typical parameters $E = 64$, $d = 4096$, $k = 2000$, this is approximately 500M operations per projection.

C Efficient Implementation and Storage

Enforcing geometric constraints on large-scale Mixture-of-Experts (MoE) models presents a unique systems challenge. While the parameter updates are sparse, the constraint matrices are dense, layer-specific, and expert-specific. Storing a dense $d \times d$ projector for every expert across all layers would require prohibitive memory. For a standard 30B model ($d = 4096$, $E = 128$, $L = 60$), naive storage would consume over 2 TB of VRAM. To resolve this, we implement a Tiered Hierarchical Caching Strategy, reducing the active memory footprint to $< 1\%$ of the model size without stalling the training pipeline.

C.1 Implicit Low-Rank Storage

Instead of instantiating and storing the full dense projector $P_{\mathcal{N}} \in \mathbb{R}^{d \times d}$, we exploit the spectral properties of the router representations. We observe that the "retain" subspace for any single expert is effectively low-rank ($k \ll d$). Consequently, we compute and store only the orthonormal basis of the null space, $U_{\text{null}} \in \mathbb{R}^{d \times k}$, derived from the Singular Value Decomposition (SVD) of the expert's input covariance (see Eq. 10). The projection operation is then performed implicitly via matrix-vector multiplication in the low-rank factorized form:

$$P_{\mathcal{N}} \nabla = (U_{\text{null}} U_{\text{null}}^T) \nabla = U_{\text{null}} (U_{\text{null}}^T \nabla) \quad (21)$$

This reduces the storage complexity per expert from $\mathcal{O}(d^2)$ to $\mathcal{O}(dk)$. For a typical rank $k \approx 50$ and hidden dimension $d = 4096$, this yields a compression ratio of $\approx 80\times$, allowing the structural constraints for thousands of experts to reside efficiently in system RAM or on disk.

C.2 Hierarchical Caching System

To manage the flow of these constraints during the unlearning optimization, we developed a custom PyTorch autograd hook (MemoryEfficientConstraintHook) that implements a three-tier cache replacement policy (LRU):

- **Tier 1: Hot Cache (VRAM).** Stores the pre-computed projectors for the currently active experts in GPU memory. Capacity is strictly limited (e.g., $C_{\text{hot}} = 8$ experts) to prevent OOM errors during the backward pass.
- **Tier 2: Warm Cache (Host RAM).** Stores compressed basis vectors (U_{null}) for frequently accessed experts in CPU memory. This tier serves as a low-latency buffer, avoiding the I/O bottleneck of disk reads.
- **Tier 3: Cold Storage (NVMe/Disk).** The complete set of expert constraints is sharded into individual files on disk. These are loaded lazily only when a "cache miss" occurs in the upper tiers.

C.3 Stochastic Fallback Mechanism

To ensure numerical stability without incurring unnecessary computation, our implementation employs an adaptive verification step. During the backward pass, the hook first applies the primary projection. It then checks the residual violation against the inequality constraints (Eq. 5). Only if the violation exceeds a numerical tolerance ($\tau > 1e^{-4}$) does the system trigger the **Randomized Kaczmarz** solver. This "lazy enforcement" ensures that the computationally intensive iterative projection (Algorithm 1) is only invoked for the small subset of gradients that actually threaten the routing stability bounds.

D Randomized Kaczmarz for Halfspace Projection

We employ the Randomized Kaczmarz (RK) algorithm to efficiently enforce the inequality constraints described in Section 4.3. Unlike standard cyclic projections, RK samples constraints with probability proportional to their geometric "importance" (squared Euclidean norms), leading to faster convergence rates.

D.1 Problem Formulation

For expert j at layer ℓ , we must find a gradient update $\tilde{\nabla}$ that satisfies the set of linear inequalities for the non-selected inputs ($i \notin \mathcal{I}_{j,\ell}$):

$$\langle \tilde{\nabla}, x_{r,\ell}^{(i)} \rangle \leq \tau_{i,j} - \varepsilon \quad (22)$$

where $\tau_{i,j}$ is the margin threshold. Let A be the matrix where rows correspond to the input vectors $x_{r,\ell}^{(i)}$ for all $i \notin \mathcal{I}_{j,\ell}$, and let b be the vector of thresholds $\tau_{i,j} - \varepsilon$.

While the classic Kaczmarz method sweeps through rows cyclically, the Randomized Kaczmarz algorithm selects a constraint index i at iteration k with probability p_i :

$$p_i = \frac{\|x_{r,\ell}^{(i)}\|_2^2}{\|A\|_F^2} \quad (23)$$

where $\|A\|_F^2 = \sum_m \|x_{r,\ell}^{(m)}\|_2^2$ is the Frobenius norm of the constraint matrix.

D.2 Algorithm

Algorithm 1 details the procedure. We precompute the row norms and sampling probabilities. At each step, we sample a constraint; if the constraint is violated, we project the current gradient estimate orthogonally onto the defining hyperplane.

Require: Router gradients $\{\nabla_{\theta_{j,\ell}\mathcal{L}}\}$, retain set $X_{r,\ell}$, expert selections $\{\mathcal{I}_{j,\ell}\}$, thresholds $\{\tau_{i,j}\}$

Ensure: Constrained gradients $\{\tilde{\nabla}_{\theta_{j,\ell}}\}$

```

1: for each layer  $\ell = 1, \dots, L$  do
2:   for each expert  $j = 1, \dots, E$  do
3:     {— Phase 1: Equality Constraints (Null Space) —}
4:      $X_{\text{eq}}^{(j)} \leftarrow [x_{r,\ell}^{(i)}]_{i \in \mathcal{I}_{j,\ell}}$ 
5:      $P_{j,\ell} \leftarrow I - X_{\text{eq}}^{(j)} (X_{\text{eq}}^{(j)T} X_{\text{eq}}^{(j)})^\dagger X_{\text{eq}}^{(j)T}$ 
6:      $\tilde{\nabla}^{(0)} \leftarrow P_{j,\ell} \nabla_{\theta_{j,\ell}\mathcal{L}}$ 
7:     {— Phase 2: Inequality Constraints (Randomized Kaczmarz) —}
8:     Let  $X_{\text{ineq}}$  be the matrix of rows  $x_{r,\ell}^{(i)}$  for  $i \notin \mathcal{I}_{j,\ell}$ 
9:     Compute row norms  $w_i = \|x_{r,\ell}^{(i)}\|_2^2$ 
10:    Compute probabilities  $p_i = w_i / \sum w$ 
11:     $k \leftarrow 0$ 
12:    while  $k < k_{\text{max}}$  do
13:      Sample index  $i$  from distribution  $p$ 
14:       $v_{i,j} \leftarrow (\tilde{\nabla}^{(k)})^T x_{r,\ell}^{(i)} - (\tau_{i,j} - \varepsilon)$  {Compute Residual}
15:      if  $v_{i,j} > 0$  then
16:         $\text{step} \leftarrow v_{i,j} / w_i$ 
17:         $\tilde{\nabla}^{(k+1)} \leftarrow \tilde{\nabla}^{(k)} - \text{step} \cdot x_{r,\ell}^{(i)}$ 
18:      else
19:         $\tilde{\nabla}^{(k+1)} \leftarrow \tilde{\nabla}^{(k)}$ 
20:      end if
21:       $k \leftarrow k + 1$ 
22:      {Optional: Early exit if converged (checked every  $N$  steps)}
23:    end while
24:     $\tilde{\nabla}_{\theta_{j,\ell}} \leftarrow \tilde{\nabla}^{(k)}$ 
25:  end for
26: end for
27: return  $\{\tilde{\nabla}_{\theta_{j,\ell}}\}$ 

```

Algorithm 1: GRIP Training-Time Enforcement via Randomized Kaczmarz

D.3 Convergence Analysis

By utilizing Randomized Kaczmarz, we improve the convergence rate significantly compared to standard cyclic projections. Strohmer and Vershynin (2009) proved that for consistent linear systems, RK converges linearly in expectation (exponential decay of error).

Theorem 1 (Convergence of Randomized Kaczmarz). *Let $\tilde{\nabla}^*$ be the projection of the initial gradient onto the feasible region. The expected error at iteration k satisfies:*

$$\mathbb{E}[\|\tilde{\nabla}^{(k)} - \tilde{\nabla}^*\|_2^2] \leq (1 - \kappa^{-2})^k \|\tilde{\nabla}^{(0)} - \tilde{\nabla}^*\|_2^2 \quad (24)$$

where κ is the scaled condition number of the constraint matrix.

This result guarantees that the algorithm rapidly reduces the error, making it highly suitable for high-dimensional gradient constraints where the number of constraints N_r is large. In contrast to the $O(1/\sqrt{k})$ rate of cyclic projections, the linear convergence $O(c^k)$ allows us to use a small fixed number of iterations ($k_{\max} \approx 100$) to achieve high precision.

D.4 Computational Complexity

The computational cost is dominated by the probability precomputation and the iterative updates:

- **Precomputation:** Computing squared norms for all non-selected inputs takes $O(d \cdot N_{\text{ineq}})$. This is done once per batch.
- **Per Iteration:** Sampling takes $O(\log N_{\text{ineq}})$ or $O(1)$ with aliasing methods. The update step involves a single dot product and vector addition: $O(d)$.
- **Total Complexity:** $O(dN_{\text{ineq}} + k_{\max}d)$.

Since k_{\max} is a small constant independent of the system size (due to the linear convergence rate), the marginal cost of enforcement scales linearly with the dimension d , which is computationally efficient for large LLM hidden states ($d \approx 4096$).

D.5 Complexity and Memory Analysis

Time Complexity Efficiency. The computational advantage of Post-Training Correction (PTC) over Training-Time Enforcement (TTE) stems from the frequency of projection operations:

- **TTE Cost:** Requires projecting gradients at every step k for every layer l . Total cost scales as $O(K \cdot L \cdot d^3)$, where K is the number of unlearning steps (typically $K \approx 2000$).
- **PTC Cost:** Requires a single analytical correction per layer after training. Total cost scales as $O(1 \cdot L \cdot d^3)$.

Since $K \gg 1$, PTC reduces the dominant computational term by three orders of magnitude, resulting in the negligible $1.21\times$ training time overhead reported in Section 4.4.

Memory and Offloading. The space complexity $O(LdN_r)$ for caching representations $X_{r,\ell}$ is structurally efficient for two reasons:

1. **Relative Size:** For a 30B parameter model, the total cache size for retain set representations ($N_r \approx 2048$) is approximately 0.5 GB in FP16. Compared to the ≈ 60 GB required to load the model weights, this constitutes less than 1% of the total memory footprint.
2. **Offloading Strategy:** Unlike gradients which must reside in VRAM for backpropagation, the cached representations $X_{r,\ell}$ are static. We implement an asynchronous pre-fetching system that streams $X_{r,\ell}$ from CPU RAM or NVMe storage only when Layer l is being corrected. This ensures zero impact on peak VRAM usage during the unlearning process.

E Security Evaluation Protocols

To rigorously quantify the robustness of unlearning, we define two formal evaluation algorithms: **Adversarial Expert Forcing**, which tests for latent knowledge retention in expert parameters, and **Side-Channel Vulnerability**, which measures information leakage through routing patterns.

E.1 Adversarial Expert Forcing

This protocol simulates a white-box adversary who bypasses the router’s suppression mechanism to directly access erased knowledge. We define the recovery rate as the accuracy of the unlearned model when forced to use the routing path of the original, pre-unlearning model.

```

1: Input: Pre-unlearning Model  $\Theta_{pre}$ , Unlearned Model  $\Theta_{post}$ , Hazardous Query Set  $\mathcal{D}_{haz}$ 
2: Output: Adversarial Recovery Rate (ARR)
3:  $N_{correct} \leftarrow 0$ 
4: for each input pair  $(x, y)$  in  $\mathcal{D}_{haz}$  do
5:   {Step 1: Extract original routing path}
6:    $\mathcal{S}_{orig} \leftarrow \text{GetActiveExperts}(\Theta_{pre}, x)$ 
7:   {Step 2: Forward pass with forced routing}
8:   {Override  $\Theta_{post}$  router to strictly use  $\mathcal{S}_{orig}$ }
9:    $\hat{y} \leftarrow \text{Forward}(\Theta_{post}, x, \text{force\_experts} = \mathcal{S}_{orig})$ 
10:  {Step 3: Measure recovery}
11:  if  $\text{argmax}(\hat{y}) = y$  then
12:     $N_{correct} \leftarrow N_{correct} + 1$ 
13:  end if
14: end for
15: return  $N_{correct}/|\mathcal{D}_{haz}|$ 

```

Algorithm 2: Adversarial Expert Forcing Evaluation

E.2 Side-Channel Vulnerability Assessment

This protocol quantifies the distinguishability of “forgotten” queries from retained queries based solely on expert activation patterns. This simulates a side-channel attack where an adversary infers query membership via timing or power analysis of specific GPU nodes in a distributed inference setting.

```

1: Input: Unlearned Model  $\Theta_{post}$ , Forget Set  $\mathcal{D}_f$ , Retain Set  $\mathcal{D}_r$ 
2: Output: Vulnerability Ratio (VR)
3: {Step 1: Construct Fingerprint Dataset}
4:  $\mathcal{X}_{probe} \leftarrow \emptyset$ 
5: for each  $x \in \mathcal{D}_f \cup \mathcal{D}_r$  do
6:    $\mathcal{S}_x \leftarrow \text{GetActiveExperts}(\Theta_{post}, x)$ 
7:    $v_{fp} \leftarrow \mathbf{0} \in \{0, 1\}^E$  {Initialize binary fingerprint vector}
8:   for each expert index  $e \in \mathcal{S}_x$  do
9:      $v_{fp}[e] \leftarrow 1$ 
10:  end for
11:   $y_{label} \leftarrow 1$  if  $x \in \mathcal{D}_f$  else 0
12:   $\mathcal{X}_{probe}.append((v_{fp}, y_{label}))$ 
13: end for
14: {Step 2: Train Attack Classifier (Logistic Regression)}
15: Split  $\mathcal{X}_{probe}$  into  $\mathcal{X}_{train}, \mathcal{X}_{test}$ 
16: Fit classifier  $\mathcal{C}$  on  $\mathcal{X}_{train}$  to predict  $y_{label}$  from  $v_{fp}$ 
17: {Step 3: Evaluate Leakage}
18: Accuracy  $\leftarrow \text{Evaluate}(\mathcal{C}, \mathcal{X}_{test})$ 
19: RandomBaseline  $\leftarrow 0.5$  {Assuming balanced  $\mathcal{D}_f, \mathcal{D}_r$ }
20: return Accuracy/RandomBaseline {VR > 1.0 implies leakage}

```

Algorithm 3: Side-Channel Leakage Quantification

F Direct Comparison with SEUF

To evaluate the efficacy of our framework against the current state-of-the-art in MoE unlearning, we perform a direct head-to-head comparison with SEUF (Sparse Expert Unlearning Framework) [27].

Experimental Setup. To ensure a strictly fair comparison, we replicate the specific experimental conditions used in the original SEUF study. We utilize the **Qwen1.5-MoE-A2.7B-Chat** architecture instead of the 30B model used in our main experiments. We evaluate performance on the **WMDP-Cyber** dataset, consistent with the hazardous knowledge removal tasks targeted by both frameworks. We compare both methods when applied to the Representation Misdirection (RMU) unlearning algorithm.

Table 7: Direct comparison with SEUF on Qwen1.5-MoE-A2.7B-Chat. ↓/↑ indicates lower/higher is better. Our results are **bolded**.

Method	FA↓	RA↑	RS↑
RMU Baseline	0.28	0.38	0.35
SEUF + RMU	0.25	0.53	0.87
Relaxed Constraint (GRIP) + RMU	0.25	0.61	0.94
PTC (GRIP) + RMU	0.27	0.63	0.99

F.1 Results and Analysis

The quantitative results are presented in Table 7. Our analysis highlights three key findings:

Unlearning Efficacy (FA): Both frameworks successfully reduce the model’s accuracy on the forget set to near-random levels. GRIP (Relaxed Constraint) achieves an FA of 0.25, matching SEUF exactly, while PTC achieves 0.27. This confirms that restricting the router’s optimization landscape via null-space projections does not hinder the model’s ability to erase hazardous knowledge.

Superior Utility Preservation (RA): GRIP demonstrates a significant advantage in retaining general model capabilities. While SEUF recovers a Retain Accuracy (RA) of 0.53, GRIP improves this to **0.61** (+15%) with relaxed constraints and **0.63** (+19%) with PTC. SEUF relies on soft regularization penalties (L_2 norms on router weights) to maintain stability. Our results suggest these soft penalties are insufficient to prevent the "optimization shortcut" described in Section 1, leading to degraded utility. In contrast, GRIP’s hard geometric constraints strictly enforce the preservation of retain-set routing, protecting general knowledge more effectively.

Routing Stability (RS): We observe that SEUF improves routing stability over the unconstrained baseline (0.87 vs 0.35) but still permits noticeable drift. GRIP eliminates this drift almost entirely, achieving an RS of **0.94** with training-time constraints and **0.99** with Post-Training Correction. This validates our hypothesis that decoupling routing stability from parameter plasticity is essential for robust MoE unlearning.